Available online at www.sciencedirect.com
ScienceDirect
Journal of Organometallic Chemistry 692 (2007) 3984–3993
Journal of Organometallic Chemistry
www.elsevier.com/locate/jorganchem

Theoretical studies of the oxidative addition of PhBr to $Pd(PX_3)_2$ and $Pd(X_2PCH_2CH_2PX_2)$ (X = Me, H, Cl)

Reza Fazaeli [a], Alireza Ariafard [b,*], Saiedeh Jamshidi [b], Elham S. Tabatabaie [b,c], Khatereh A. Pishro [c]

[a] Department of Chemistry, Islamic Azad University, South Tehran Branch, Tehran, Iran
[b] Department of Chemistry, Faculty of Science, Central Tehran Branch, Islamic Azad University, Felestin Square, Tehran, Iran
[c] Central Tehran Branch Chemical Society, Faculty of Science, Central Tehran Branch, Islamic Azad University, Felestin Square, Tehran, Iran

Received 22 February 2007; received in revised form 20 May 2007; accepted 5 June 2007
Available online 15 June 2007

Abstract

The density functional theory calculations were used to study the influence of the substituent at P on the oxidative addition of PhBr to $Pd(PX_3)_2$ and $Pd(X_2PCH_2CH_2PX_2)$ where X = Me, H, Cl. It was shown that the C_{ipso}–Br activation energy by $Pd(PX_3)_2$ correlates well with the rigidity of the X_3P–Pd–PX_3 angle and increases via the trend X = Cl < H < Me. The more rigid the X_3P–Pd–PX_3 angle is, the higher the oxidative addition barrier is. The exothermicity of this reaction also increases via the same sequence X = Cl < H < Me. The trend in the exothermicity is a result of the Pd(II)–PX_3 bond strength increasing faster than the Pd(0)–PX_3 bond strength upon going from X = Cl to Me. Contrary to the trend in the barrier to the oxidative addition of PhBr to $Pd(PX_3)_2$, the C_{ipso}–Br activation energy by $Pd(X_2PCH_2CH_2PX_2)$ decreases in the following order X = Cl > H > Me. This trend correlates well with the filled d_π orbital energy of the metal center. For a given X, the oxidative addition reaction energy was found to be more exothermic for the case of $X_2PCH_2CH_2PX_2$ than for the case of PX_3. This effect is especially more important for the strong electron donating phosphine ligands (X = Me) than for the weak electron donating phosphine ligands (X = Cl).

Keywords: Density functional theory calculations; Oxidative addition; Palladium

1. Introduction

It has been established that oxidative addition of organic halides (RX) to $Pd(0)L_n$ ($n = 1, 2$) species is the first step in the many Pd-catalyzed cross-coupling reactions, where L is typically a phosphine ligand and X is a halide [1–3]. The generally accepted mechanism involves the concerted addition of RX to $Pd(0)L_n$ via a three center transition state leading to the fission of R–X bond and the generation of Pd–R and Pd–X bonds [4]. As shown in Scheme 1, in the transition state, the filled σ_{R-X} orbital of RX interacts with the vacant sp_σ-hybridized orbital of metal. There is also a second interaction between the filled d_π orbital of metal and the vacant σ^*_{R-X} orbital of RX leading to the breaking of the R–X bond. Thus, one can expect that a strong σ-donor phosphine ligand, which can increase the electron density of metal, would facilitate oxidative addition reaction through the stronger charge transfer from the d_π orbital of metal to the σ^*_{R-X} orbital of RX.

Recently, many experimental [5] and theoretical [6–8] works have been employed to investigate the activation of the C–X bonds by coordinatively unsaturated active species $Pd(0)L_n$. However, a proper understanding of how the electronic feature of ancillary ligand L influences the reactivity of RX is still lacking. To provide a deeper insight into how the L ligand affects the oxidative addition reaction of organic halides, we investigate the model oxidative addition reaction between PhBr and $Pd(PX_3)_2$ (X = Me, H, Cl) with the aid of B3LYP density functional theory

* Corresponding author.
E-mail address: ariafard@yahoo.com (A. Ariafard).

0022-328X/$ - see front matter © 2007 Elsevier B.V. All rights reserved.
doi:10.1016/j.jorganchem.2007.06.011

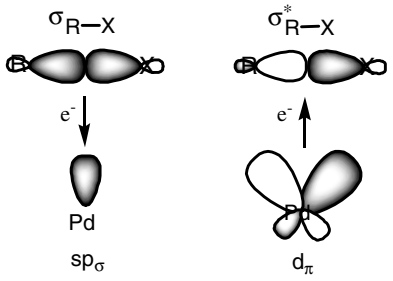

Scheme 1.

(DFT) calculations. The representative set of PX_3 includes the ligand with gradually changing donor and acceptor characters. The σ-donor character of PX_3 varies as follows: $PMe_3 > PH_3 > PCl_3$ while the π-acceptor character of PX_3 increases in the order $PMe_3 < PH_3 < PCl_3$ [9]. According to Tolman's map [10], PCl_3 was chosen to electronically model weak bases such as $P(OC_6H_4CN)_3$ (**I**). We also theoretically investigated the effect of different chelating phosphine ligands on oxidative addition of PhBr to $Pd(X_2PCH_2CH_2PX_2)$ (X = Me, H, Cl).

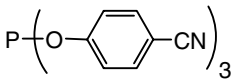

I

2. Computational detail

GAUSSIAN 98 [11] was used to fully optimize all the structures reported in this paper at the B3LYP [12] level of density functional theory. The effective core potentials of Hay and Wadt with double-ζ valance basis sets (LanL2DZ) [13] were chosen to describe Pd, P, Br and Cl. The 6-31G basis set was used for other atoms [14]. Polarization functions were also added for C($\zeta_d = 0.6$), Cl($\zeta_d = 0.514$), Br($\zeta_d = 0.389$) and P($\zeta_d = 0.340$) [15]. Frequency calculations at the same level of theory have also been performed to identify all of the stationary points as minima (zero imaginary frequencies) or transition states (one imaginary frequency), and to compute free energies in the gas phase at 298.15 K and 1 atm, which include entropic contributions by taking into account the vibrational, rotational, and translational motions of the species under consideration. Chemically more interesting ΔG values were used in the discussion, and corresponding ΔE values were given in parentheses. Partial atomic charges were calculated on the basis of the natural bond orbital (NBO) analyses [16].

To test the accuracy of the medium-size basis set (BS1) used, we carried out single point energy calculations for several selected structures by using a larger basis set: SDDALL for Pd and 6-311G** for all other atoms. We also added an f polarization function of 1.472 [17] to SDDALL [18] for Pd. This basis set will be referred to as BS2. These additional calculations show that the basis set dependence is small. For example, using the smaller basis set (BS1), the

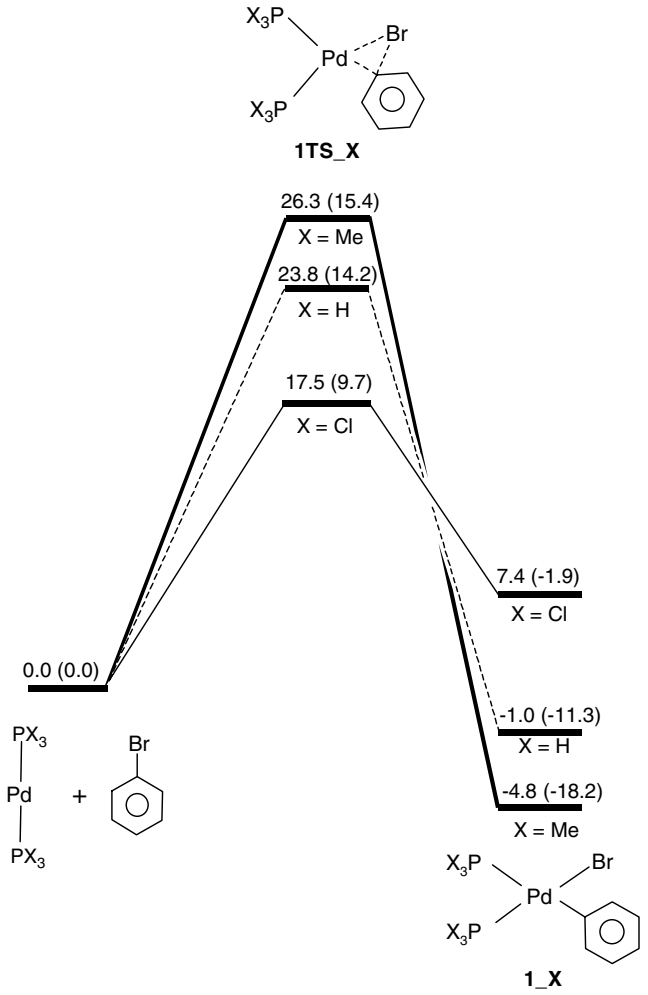

Fig. 1. Potential energy profiles calculated for the oxidative addition of PhBr to $Pd(PX_3)_2$ (X = Me, H, Cl). Gibbs free energies at 1 atm, 298.15 K and electronic energies (in parentheses) relative to the $Pd(PX_3)_2$ and PhBr fragments are given in kcal/mol.

relative energies of **1TS_Me**, **1TS_H**, and **1TS_Cl** (Fig. 1) are 15.4, 14.2, and 9.7 kcal/mol, respectively. Using the larger basis set (BS2), the relative energies are 17.0, 15.1, and 9.8 kcal/mol, respectively. Using the smaller basis set (BS1), the relative energies of **2TS_Me**, **2TS_H**, and **2TS_Cl** (Fig. 5) are −0.3, 1.2, and 6.2 kcal/mol, respectively. Using the larger basis set (BS2), the relative energies are −1.1, 0.8, and 4.1 kcal/mol, respectively.

Charge decomposition analyses (CDA) were calculated on optimized geometries at the same level of theory for structural optimization [19]. In the CDA [20] scheme, the orbital contributions to the charge distributions of the complex and the two fragments that define the bond of interest are divided into four parts: (i) the donation from occupied donor fragment orbitals to vacant orbitals on the acceptor fragment (d) (ii) the back-donation from occupied orbitals on the acceptor fragment to vacant orbitals on the donor fragment (b), (iii) the repulsive polarization of occupied orbitals on both the fragments (r) and (iv) the residual term (s) which should be approximately zero for true donor–acceptor complexes.

3. Results and discussion

3.1. Oxidative addition transition state of the reaction $Pd(PX_3)_2 + PhBr \rightarrow (PX_3)_2Pd(Ph)(Br)$

The calculated energy profiles for the oxidative addition of PhBr, on the basis of a S_NAr type mechanism [5k,8a], are shown in Fig. 1. Analysis of the results given in Fig. 1 clearly shows that upon going from PMe_3 to PH_3 and to PCl_3, the activation barrier becomes lower and the complex **1_X** becomes less stable relative to the corresponding free reactants. These results are quite unexpected because $Pd(PCl_3)_2$, which has phosphine ligands of low donicity, has lower oxidative addition barrier than $Pd(PH_3)_2$, while $Pd(PMe_3)_2$, which has phosphine ligands of high donicity, has higher oxidative addition barrier than $Pd(PH_3)_2$. It also follows from Fig. 1 that the higher activation barrier for $Pd(PMe_3)_2$ compared to $Pd(PH_3)_2$ and $Pd(PCl_3)_2$ cannot be explained from a thermodynamic view point since the trend found in the activation barriers does not follow the same trend as in the oxidative addition reaction energies.

Examination of the structural parameters for the oxidative addition transition sates shown in Fig. 2 does not give us a clue behind why PMe_3 as ancillary ligands disfavors kinetically the oxidative addition reaction. In the case of PMe_3, the geometry of $Pd(PMe_3)_2$ is distorted only to a medium extent in the transition sate; the angle between the phosphines is reduced to 118.3°. In contrast, the geometry distortions of $Pd(PX_3)_2$, where X = H and Cl, in the transition states are larger. The angles between the phosphines are calculated as 111.4° and 102.2° for **1TS_H** and **1TS_Cl**, respectively. The C_{ipso}–Br distance progressively increases as one goes from **1TS_Me** to **1TS_Cl**. In **1TS_Me**, PhBr is farther away from the metal center than in both the transition states **1TS_H** and **1TS_Cl**. On the basis of the results, an "earlier" transition state is suggested for **1TS_Me** as compared to **1TS_H** and **1TS_Cl**, although the activation barrier is considerably higher for the case of PMe_3 [21].

To understand the effect of substituents at the P atom on the relative stability of the transition states, we analyzed **1TS_Me**, **1TS_H** and **1TS_Cl** using the energy decomposition analysis, based on the activation strain model [22], as shown in Scheme 2. In the scheme, the deformation energies ΔE_{def} (1) and ΔE_{def} (2) represent the energy required to deform the $Pd(PX_3)_2$ and PhBr reactants, respectively,

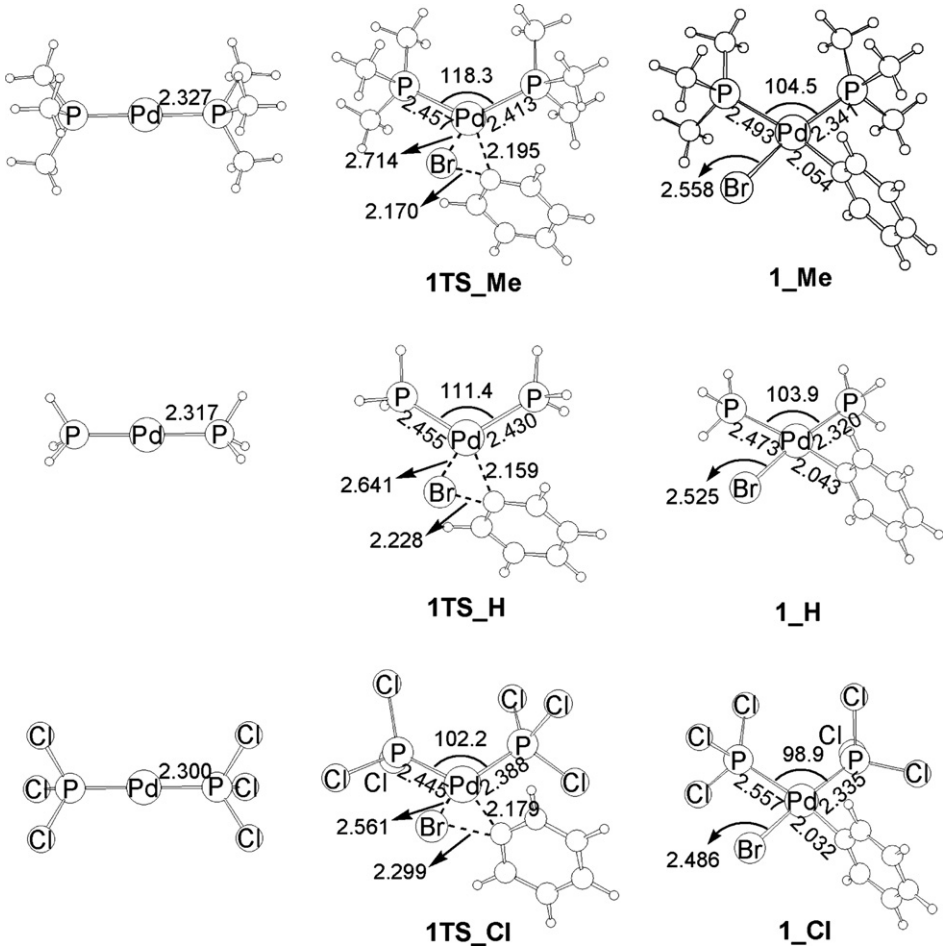

Fig. 2. Calculated structures for species involved in the oxidative addition of PhBr to $Pd(PX_3)_2$ (X = Me, H, Cl). Selected bond distances and angles are given in angstroms and degree, respectively.

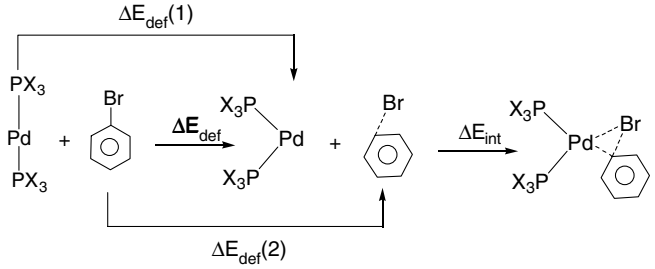

	$\Delta E_{def}(1)$ kcal/mol	$\Delta E_{def}(2)$ kcal/mol	ΔE_{int} kcal/mol
X = Me	15.1	16.2	-15.8
X = H	14.4	19.4	-19.5
X = Cl	9.4	23.8	-23.4

Scheme 2.

Table 1
Bond distance, relative energy, and molecular orbital (MO) energies of the $Pd(PX_3)_2$ with a variety of angle θ

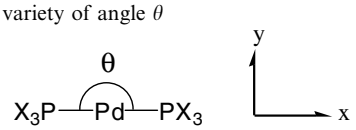

X	θ (°)	Pd–P distance (Å)	Relative energy (kcal/mol)	d_{xy} energy (eV)	$d_{x^2-y^2}$ energy (eV)	LUMO energy (eV)
Me	180.0	2.326	0.0	−5.33	−4.16	0.01
	120.0	2.345	10.5	−4.22	−5.33	−0.27
	100.0	2.385	18.9	−3.86	−5.47	−0.52
H	180.0	2.316	0.0	−6.09	−5.01	−0.38
	120.0	2.327	7.4	−5.17	−6.07	−0.68
	100.0	2.349	12.6	−4.92	−6.28	−0.87
Cl	180.0	2.300	0.0	−7.94	−6.50	−2.64
	120.0	2.298	1.5	−6.91	−8.08	−2.80
	100.0	2.333	6.4	−6.53	−8.27	−2.88

to the geometries they have in the transition states. The interaction energy between the deformed PhBr and $Pd(PX_3)_2$ reactants in the transition state is denoted by ΔE_{int}. The trend calculated for ΔE_{def} (2) can be reflected in the trend calculated for the elongation of the C_{ipso}–Br distance at the transition states (Fig. 2). Upon going from X = Me to Cl, ΔE_{int} becomes more negative, likely due to that **1TS_Me** is an "earlier" transition state, while **1TS_Cl** is a "late" transition state. Interestingly, for each of the transition sates, the sum of ΔE_{def} (2) and ΔE_{int} remains nearly constant. Thus, the difference in the oxidative addition reaction barriers can be easily understood through the difference in the deformation energies ΔE_{def} (1). It follows from the results that the rigidity of the X_3P–Pd–PX_3 angle would decrease as one goes from X = Me to Cl. To further support the argument here, we performed a partial geometry optimization by fixing the X_3P–Pd–PX_3 bite angle at 120 ° and 100 ° (Table 1). The calculations reveal that, in a bent geometry, the relative instability of $Pd(PX_3)_2$ increases as the X_3P–Pd–PX_3 bite angles decreases. For a given bite angle, the relative instability of $Pd(PX_3)_2$ increases in the order X = Cl < H < Me, indicating that the bending of X_3P–Pd–PX_3 angle from 180° for more basic ancillary ligands is more difficult than that for less basic ancillary ligands.

Fig. 3 shows the correlation diagram of the important metal orbitals for changing the X_3P–Pd–PX_3 angle. For a linear geometry, the d_{xy} orbital is stabilized by metal-to-PX_3 back-donation interaction. The HOMO, which is $d_{x^2-y^2}$ in character, mainly remains nonbonding. For a bent geometry, the $d_{x^2-y^2}$ orbital is stabilized by back-bonding to the PX_3 groups. The bending of the X_3P–Pd–PX_3 angle causes the d_{xy} orbital to be the HOMO, because the bending turns on a slight σ^*-antibonding interaction between d_{xy} and the P lone pair. Thus, the more basic the ancillary ligands, the more the repulsive interaction, the more destabilized the bent geometry. The repulsive interaction is

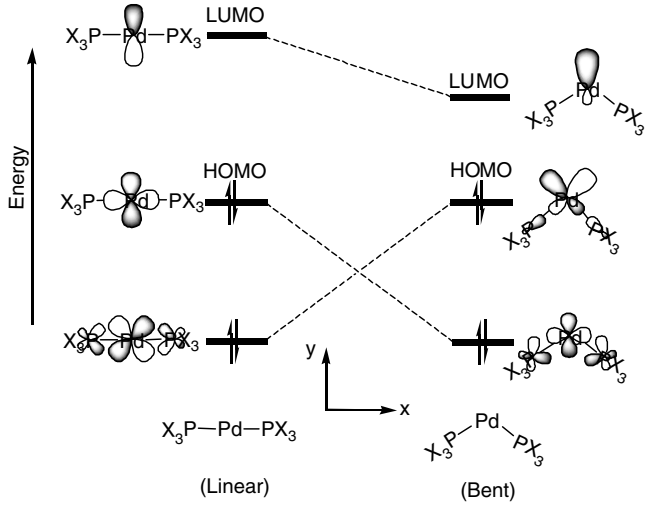

Fig. 3. Schematic orbital correlation diagram for the selected molecular orbitals of the linear and bent structures of $Pd(PX_3)_2$.

reflected in the change of the Pd–PX_3 distances. The Pd–PX_3 distances are elongated as the X_3P–Pd–PX_3 angle decreases (Table 1). The LUMO in a bent structure is stabilized compared to that in a linear structure and becomes a sp_y-hybridized orbital.

As mentioned in Section 1, the key interaction leading to the breaking of the Ph–Br bond is charge transfer from the metal d_π orbital to a proper vacant orbital of PhBr. The electron donating PMe_3 ligand destabilizes the HOMO (d_{xy} orbital) of the bent $Pd(PX_3)_2$ fragment and making it more available for back donation (Table 1). Thus, one might have expected that the PMe_3 ligands would facilitate the oxidative addition reaction. Although, the energy required distorting the ancillary bite angle from 180° is the largest for the case of PMe_3. On the contrary, the HOMO for the case of PCl_3 is lying lower in energy than

that for the case of PMe_3 (Table 1), while the distortion energy for PCl_3 is the smallest. From these results, one may conclude that the barrier to the oxidative addition reaction of PhBr to linear $Pd(PX_3)_2$ is mainly reliant on the rigidity of the X_3P–Pd–PX_3 angle. In other words, the distortion energy ΔE_{def} (1) is a determining factor of the activation barriers.

3.2. Oxidative addition product of the reaction $Pd(PX_3)_2 + PhBr \rightarrow (PX_3)_2Pd(Ph)(Br)$

As mentioned above, RX reacts with PdL_2 by a three centered transition state, giving rise to a *cis*-$(L)_2Pd(R)(X)$ complex. The *cis*-isomer has been seldom isolated and it is usually believed that it rapidly isomerizes to the *trans*-isomer [5e,23]. Thus, it seems reasonable if we assume the *trans*-isomer as the product of the oxidative addition reaction. It is also obvious that comparison of structural features and energetics between the reactant, $Pd(PX_3)_2$, and the corresponding *trans*-isomer is much more convenient than that between the reactant and the corresponding *cis*-isomer, because in the former, both the Pd–phosphine bonds are in a *trans* arrangement.

Our calculations on the *cis*- and *trans*-isomers of $(PX_3)_2Pd(R)(Br)$, where X = Me and H, show that in agreement with the general observation, the *trans*-isomers are more stable. For the case of PCl_3, the *trans*-isomer is calculated to be slightly less stable than the *cis*-isomer (Figs. 1 and 4). The inter-conversion mechanism between *cis*- and *trans*-isomers is not addressed here because it has previously been the subject of several theoretical studies [6c,8c].

Regardless what the product is, the reaction free energy for the oxidative addition of PhBr to $Pd(PX_3)_2$ decreases in the order X = Me > H > Cl, indicating that stronger electron donating phosphine ligands make the oxidative addition reaction more favorable thermodynamically. Isodesmic reactions shown in Schemes 3 and 4 were used to probe the origin of why the C_{ipso}–Br bond activation by $Pd(PMe_3)_2$ is thermodynamically much more favored over the C_{ipso}–Br bond activation by $Pd(PCl_3)_2$. On the basis of

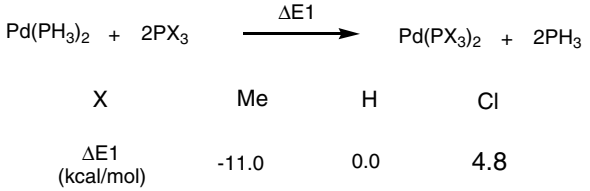

Scheme 3.

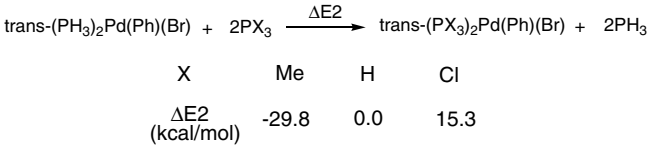

Scheme 4.

the designed isodesmic reactions, we are able to estimate the binding energies of different phosphines relative to that of PH_3. The results show that the strongest bindings belong to PMe_3 while the weakest bindings belong to PCl_3. Therefore, it is likely to conclude that the phosphine-to-Pd σ-donation is dominating bonding mode regardless of the nature of the oxidation sate of Pd. However, from Schemes 3 and 4, one can easily find that the values of $\Delta E1$ span a relatively small range from −11.0 kcal/mol (X = Me) to 4.8 kcal/mol (X = Cl), while the values of $\Delta E2$ span a relatively large range from −29.8 kcal/mol (X = Me) to 15.3 kcal/mol (X = Cl). These results suggest that, for the Pd(0) complexes, although the phosphine-to-Pd σ-donation is the dominating bonding mode, the Pd-to-phosphine π-back donation also plays an important role in the Pd(0)-phosphine bonding.

To support the claim above, we inspected the metal–ligand donor–acceptor interactions using the charge-decomposition analysis (CDA) (Table 2). The low value of the residual term(s) obtained in this study indicates that the Pd–phosphine bond is a donor–acceptor interaction and therefore the CDA scheme is appropriate for analysis. For both the Pd(0) and Pd(II) complexes, the phosphine-to-Pd σ-donation does decrease from X = Me to Cl pro-

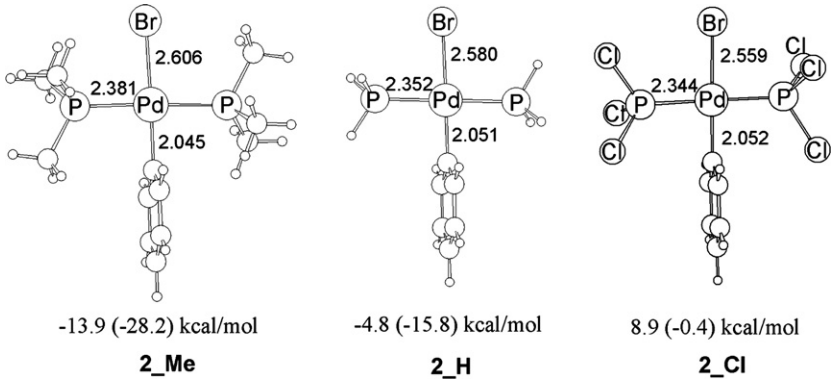

Fig. 4. Optimized structures of **2_X** together with their relative energies. Selected bond distances and angles are given in angstroms and degree, respectively.

Table 2
Results of charge decomposition analysis (CDA) on the model systems $Pd(PX_3)_2$ and *trans*-$(PX_3)_2Pd(Ph)(Br)$

Complexes	X	*d*	*b*	*b*/*d*	*r*	*s*
$Pd(PX_3)_2$	Me	0.427	0.184	0.437	−0.170	−0.018
	H	0.347	0.201	0.579	−0.162	−0.004
	Cl	0.229	0.221	0.965	−0.156	0.000
trans-$(PX_3)_2Pd(Ph)(Br)$	Me	0.500	0.170	0.340	−0.282	−0.005
	H	0.415	0.170	0.409	−0.265	0.006
	Cl	0.274	0.194	0.708	−0.302	0.009

$PX_3 \rightarrow Pd$ donation *d*, $PX_3 \leftarrow Pd$ back-donation *b*, ratio *d*/*b*, and $PH_3 \leftrightarrow Pd$ repulsive polarization *r*.

viding quantitatively support to the previous suggestion that the phosphine electron-donating ability decreases with the trend $PMe_3 > PH_3 > PCl_3$. The extent of the $PX_3 \rightarrow Pd$ donation for the Pd(II) complexes is noticeably larger than that for the corresponding Pd(0) complexes. This can be explained by the fact that the unoccupied hybridized orbital of Pd(II), which is capable accepting electron from the phosphine lone pair, is energetically lower-lying than that of Pd(0). For example, from our calculations the unoccupied orbital for the optimized fragments $(PH_3)Pd(Ph)(Br)$ and $Pd(PH_3)$ are −2.94 and −1.47 eV, respectively. In contrast, CDA data clearly indicate that $PX_3 \leftarrow Pd$ π-back donation for the Pd(0) complexes is larger than that for the corresponding Pd(II) complexes. This trend results from destabilization of the occupied d_π orbital of Pd(0) in comparison with that of Pd(II). For example, from our calculations the d_π orbital for the optimized fragments $Pd(PH_3)$ and $(PH_3)Pd(Ph)(Br)$ are −5.96 and −8.30 eV, respectively. In both the systems, the *b*/*d* ratio [24] increases upon going from X = Me to Cl indicating that PCl_3 is actually a stronger charge acceptor than PH_3 while PMe_3 is the weakest acceptor ligand. The results presented here demonstrate that the $PX_3 \leftarrow Pd$ π-back donation significantly contributes to the Pd–PX_3 interaction in the Pd(0) complexes whereas it has a lessened contribution to the Pd–PX_3 interaction in the Pd(II) complexes.

From the above results, it can be concluded that the π-accepting ability of PCl_3 relatively stabilizes $Pd(PCl_3)_2$ + PhBr more than $(PCl_3)_2Pd(Ph)(Br)$ and consequently decreases the free reaction energy. In contrast, the larger exothermicity for the reaction $Pd(PMe_3)_2 + PhBr \rightarrow (PMe_3)_2Pd(Ph)(Br)$ can be explained by the strong σ-donating ability of PMe_3 which leads to the much higher stability of the product relative to the reactants. In summary, we want to stress that the donation is usually the dominant factor in complexation with Pd(II) complexes, which is promoted by electron-donating phosphine ligands, while for Pd(0) complexes, despite the donation, the back-donation also plays an important role in the Pd–phosphine bonding.

Here, it should be mentioned that there is no correlation between the Pd–P bond distances and the relative binding energies (Figs. 2 and 4). The Pd–PMe_3 bonds having the strongest binding energies have the longest lengths. A similar trend was also observed in theoretical studies on nature of the M–PX_3 bond in $M(CO)_5PX_3$ complexes (M = Cr, Mo, W; X = H, Me, F, Cl) [9b].

3.3. Effect of chelating phosphines on oxidative addition of PhBr

The model phosphines, 1,2-bis(dimethylphosphino)ethane, 1,2-diphosphinoethane, and 1,2-bis(dichlorophosphino)ethane, were used in calculations to mimic the effect of chelating phosphines on oxidative addition of PhBr. The calculated energy profiles for the oxidative addition reaction are shown in Fig. 5. Contrary to the trend we found for the oxidative addition of PhBr to $Pd(PX_3)_2$, the overall activation barrier for the oxidative addition reaction of PhBr to $Pd(X_2PCH_2CH_2PX_2)$ decreases in the following order X = Cl > H > Me. These results are consistent with the belief that a strong electron-donating ligand on the metal center accelerates oxidative addition of organic electrophiles (RX) [25]. An comparison of the energy profiles shown in Figs. 1 and 5 demonstrates that the chelating phosphine ligands on Pd(0) favor oxidative addition, in terms of both the activation barrier and the reaction free energy. This trend is in agreement with the

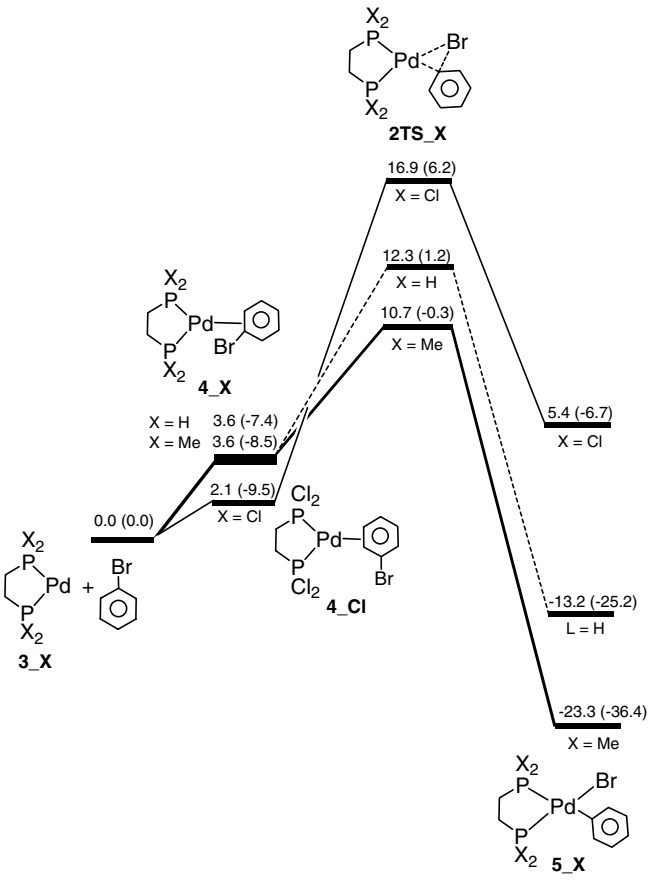

Fig. 5. Potential energy profiles calculated for the oxidative addition of PhBr to $Pd(X_2PCH_2CH_2PX_2)$ (X = Me, H, Cl). Gibbs free energies at 1 atm, 298.15 K and electronic energies (in parentheses) relative to the $Pd(PX_2CH_2CH_2PX_2)$ and PhBr fragments are given in kcal/mol.

general rule that RX oxidative addition to chelated phosphine complexes is both kinetically and thermodynamically more favorable than that to bis-phosphine complexes $Pd(PX_3)_2$ [6b,26]. However, it should be noted that, from our calculations, the effect for a strong electron donating bidentate ligand is much more considerable than the effect for a weak electron donating bidentate ligand.

The calculated trend in the stability of the transition states **2TS_X** can be explained by decomposing the activation barriers for the oxidative addition reactions according to the equation shown in Scheme 5. The deformation energies $\Delta E'_{\text{deform}}(1)$ are notably small and do not change significantly upon going from X = Me to Cl. This is understandable, if one considers the fact that the P–Pd–P angles in the Pd(0) reactants are already bent and constrained at a angle less than 98° by chelation of the phosphine (Fig. 6). Thus, in the transition states, the interaction of PhBr with the reactants produces a little distortion in the P–Pd–P angles. An comparison of the energy decomposition analyses shown in Schemes 2 and 5 also reveals that the low energy required for the reorganization of $Pd(X_2PCH_2CH_2PX_2)$ is the main reason for the low activation barrier for the oxidative addition reaction **3_X** + PhBr → **5_X**.

From Scheme 5, it is also evident that the deformation energy $\Delta E'_{\text{deform}}(2)$ increases upon going from X = Me to Cl while the interaction energies $\Delta E'_{\text{int}}$ for all the transition states are comparable. Clearly, it is mainly the relatively large deformation energy $\Delta E'_{\text{deform}}(2)$ for the case of $Cl_2PCH_2CH_2PCl_2$ that gives higher activation barrier for **3_Cl** + PhBr → **5_Cl** as compared to **3_H** + PhBr → **5_H** and **3_Me** + PhBr → **5_Me**. The reason for the large deformation energy $\Delta E'_{\text{deform}}(2)$ is easily interpreted in terms of the charge transfer from the palladium d_π orbital to the vacant Ph–Br σ^* and π^* hybrid orbital [7a]. Since the energy of palladium d_π orbital (HOMO) decreases in the series **3_Me** > **3_H** > **3_Cl** (Fig. 7), the C_{ipso}–Br bond elongation for the case of $Cl_2PCH_2CH_2PCl_2$ must occur much more significantly in order to lower the C–Br antibonding hybrid orbital in energy so as to form more efficiently the charge transfer. A larger elongation in the C_{ipso}–Br distance (Fig. 5) gives a greater deformation energy $\Delta E'_{\text{deform}}(2)$, which in turn leads to a higher activation barrier.

In the transition states, the Pd–C_{ipso} distance significantly increases in the order X = Me < H < Cl. The opposite trend, however, is observed for the Pd–Br distance. The Pd–Br distance is the longest in **2TS_Me** and the shortest in **2TS_Cl** (Fig. 6). As mentioned above, the oxidative addition reactions proceed through a S_NAr type mechanism and, in the transition states, the Pd(0) metal center plays a dual role as a electron acceptor and a electron donor during the charge transfer process. Since the palladium d_π orbital (HOMO) for the reactant **3_Me** is higher in energy than that for the reactants **3_H** and **3_Cl** (Fig. 7), the charge transfer from Pd to C_{ipso} for the former is more facile than that for the latter species. Hence, in comparison with **2TS_H** and **2TS_Cl**, the shortening of the Pd–C_{ipso} distance in **2TS_Me** is mainly due to the stronger back-donation interaction between the palladium d_π orbital and the Ph–Br σ^* and π^* hybrid orbital. In contrast, the vacant sp_σ-hybridized orbital (LUMO) for the reactant $Pd(Cl_2PCH_2CH_2PCl_2)$ is more capable of accepting the electrons from PhBr, especially from the electron lone pair of Br, than that for the reactants $Pd(H_2PCH_2CH_2PH_2)$ and $Pd(Me_2PCH_2CH_2PMe_2)$, because the former has a low lying sp_σ-hybridized orbital (Fig. 7). This electronic feature in **2TS_X** results in the shortening of the Pd–Br distance along the series X = Me > H > Cl. This balancing effect of σ-donation and π-back donation on the bonding interaction between PhBr and palladium in the oxidative addition transition states may also explain why the interaction energies $\Delta E'_{\text{int}}$ remain almost unchanged along the series from X = Me to Cl (Scheme 5).

The qualitative arguments above find support from a natural population analysis. The calculations show that PhBr gains 0.363e, 0.308e, and 0.249e from $Pd(Me_2PCH_2CH_2PMe_2)$, $Pd(H_2PCH_2CH_2PH_2)$, and $Pd(Cl_2PCH_2CH_2PCl_2)$, respectively, indicating that the back bonding interaction from Pd(d) to the Ph–Br antibonding orbital(s) dominates in the transition states. The phenyl moiety in **2TS_X** is negatively charged due to back-donation and becomes much less negative as X goes from Me to Cl (−0.218 for X = Me, −0.161 for X = H, and −0.084 for X = Cl). The sum of lone pair orbital populations of Br gradually decreases as one moves from **2TS_Me** (5.895e) to **2TS_H** (5.892e) and then to **2TS_Cl** (5.877e).

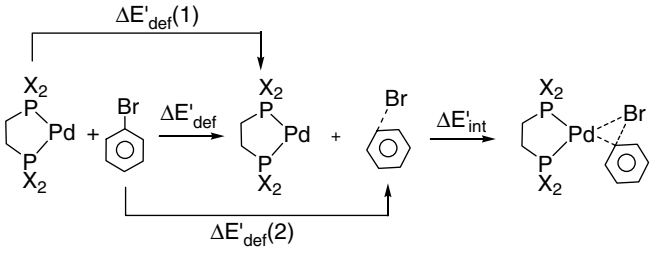

	$\Delta E'_{\text{def}}(1)$ kcal/md	$\Delta E'_{\text{def}}(2)$ kcal/mol	$\Delta E'_{\text{int}}$ kcal/mol
X = Me	4.8	16.8	-21.6
X = H	4.5	17.9	-21.2
X = Cl	4.3	23.4	-21.5

Scheme 5.

3.4. Comparison between oxidative addition reaction energy of PhBr to $Pd(PX_3)_2$ and $Pd(X_2PdCH_2CH_2PX_2)$

As noted above, it is well known that the oxidative addition reaction energy for bent PdL_2 systems dictated by chelating phosphine ligand is larger than that for the linear PdL_2 species. Our calculations, especially for the strong electron donating phosphine ligands, are consistent with the belief. The reaction free energy difference between $Pd(PX_3)_2$ + PhBr → **1_X** and **3_X** + PhBr → **5_X**

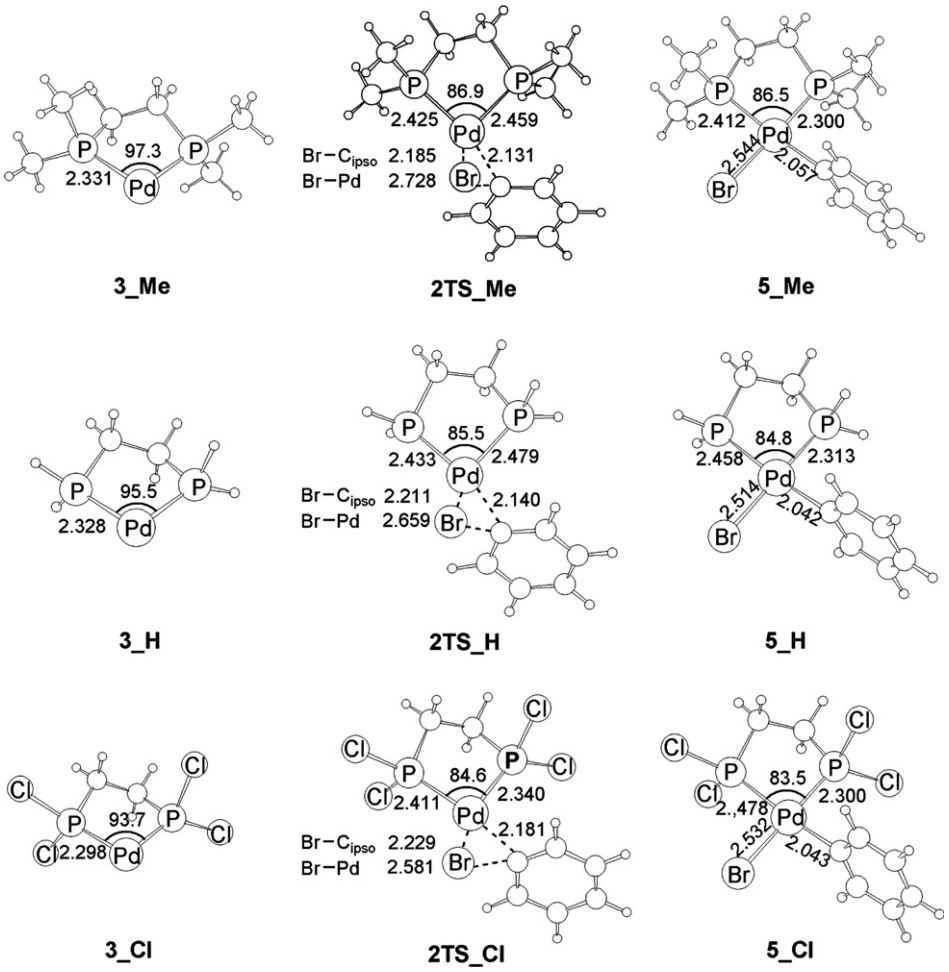

Fig. 6. Calculated structures for species involved in the oxidative addition of PhBr to Pd($X_2PCH_2CH_2PX_2$) (X = Me, H, Cl). Selected bond distances and angles are given in angstroms and degree, respectively.

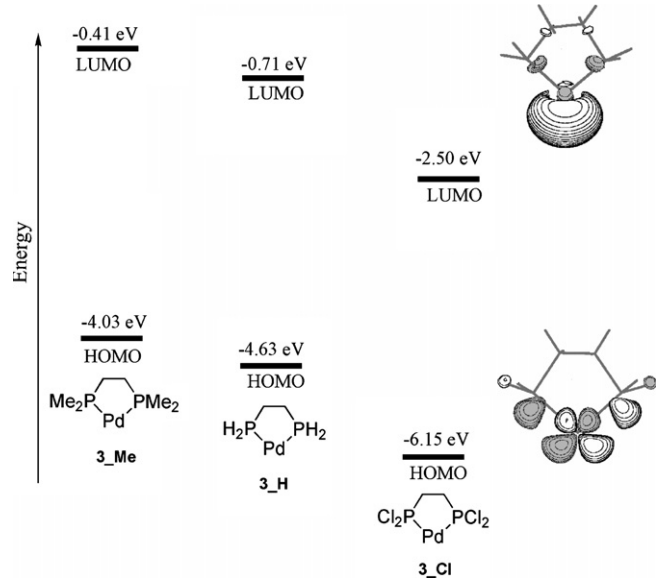

Fig. 7. Frontier orbitals of **3_Me**, **3_H** and **3_Cl**.

is calculated to be 18.5, 12.2, and 2.0 kcal/mol for X = Me, H, and Cl, respectively (Figs. 1 and 4). To provide a better understanding of what factor is responsible for the difference we designed the isodesmic reactions shown in Schemes 6 and 7. According to the equation shown in Scheme 6, for the Pd(0) complexes, ligand exchange of $2PX_3$ with $X_2PCH_2CH_2PX_2$ is an endothermic process. In particular, the exchange of $2PMe_3$ with $Me_2PCH_2CH_2PMe_2$ leads to considerable destabilization (18.4 kcal/mol). The least destabilizing process (2.1 kcal/mol) is the exchange of $2PCl_3$ with $Cl_2PCH_2CH_2PCl_2$. This result can be explained in terms of the rigidity of the X_3P–Pd–PX_3 angle which increases in the order X = Cl < H < Me. For the Pd(II) complexes, the $\Delta E4$ values are close to zero and their variations are negligible upon going from X = Me to Cl (Scheme 7). Therefore, it is the instability of **3_Me** and

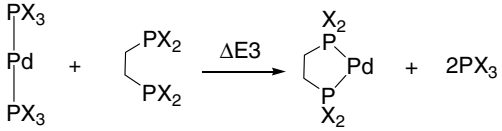

X	Me	H	Cl
ΔE3 (kcal/mol)	18.4	13.8	2.1

Scheme 6.

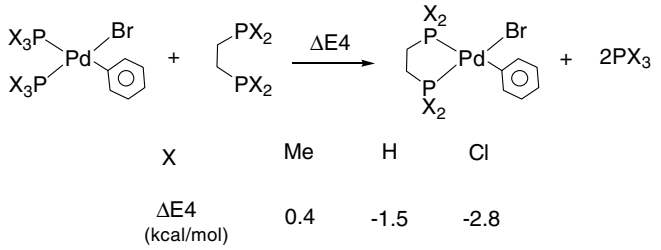

Scheme 7.

3_H relative to $Pd(PMe_3)_2$ and $Pd(PH_3)_2$ which primarily controls the reaction energy. In other words, the increase in the reaction energy for the case having a small bite angle is due to a destabilization of the reactants with respect to the corresponding products.

4. Conclusion

Several important conclusions can be drawn from the results of the calculations as described below.

1. The barrier to the oxidative addition reaction of PhBr to linear $Pd(PX_3)_2$ decreases in the order X = Me > H > Cl, indicating that the C_{ipso}–Br activation energy by $Pd(PX_3)_2$ is mainly reliant on the rigidity of the X_3P–Pd–PX_3 angle.
2. The more strongly electron donating the ligand PX_3 is, the larger the exothermicity of the oxidative addition reaction is. This result was explained as follows. The donation is usually the dominant factor in complexation with Pd(II) complexes, which is promoted by electron-donating phosphine ligands, while for Pd(0) complexes, despite the donation, the back-donation also plays an important role in the Pd–phosphine bonding.
3. Contrary to the trend in the barrier to the oxidative addition of PhBr to $Pd(PX_3)_2$, the C_{ipso}–Br activation energy by $Pd(X_2PCH_2CH_2PX_2)$ decreases in the following order X = Cl > H > Me. This trend correlates well with the filled d_π orbital energy of the metal center. The strong electron-donating phosphine ligands destabilize the filled d_π orbital and consequently facilitate the charge transfer during the oxidative addition reaction.
4. For a given X, the oxidative addition reaction energy was found to be more exothermic for the case of $X_2PCH_2CH_2PX_2$ than for the case of PX_3. This effect is especially more important for the strong electron donating phosphine ligands (X = Me) than for the weak electron donating phosphine ligands (X = Cl). This trend was explained in terms of the rigidity of the X_3P–Pd–PX_3 angle which increases in the order X = Cl < H < Me.

Acknowledgment

We acknowledge financial support from Islamic Azad University, South Tehran Branch and Central Tehran Branch.

References

[1] (a) P. Espinet, A.M. Echavarren, Angew. Chem., Int. Ed. Engl. 43 (2004) 4704;
(b) I.P. Beletskaya, A.V. Cheprakov, Chem. Rev. 100 (2000) 3009;
(c) G.T. Crisp, Chem. Soc. Rev. 27 (1998) 427;
(d) N. Miyaura, A. Suzuki, Chem. Rev. 95 (1995) 2457;
(e) A. de Meijere, F.E. Meyer, Angew. Chem., Int. Ed. Engl. 33 (1994) 2379;
(f) J.K. Stille, Angew. Chem. Int. Ed. 25 (1986) 508.
[2] (a) U. Christmann, R. Vilar, Angew. Chem. Int. Ed. 44 (2005) 366;
(b) A. Beeby, S. Bettington, I.J.S. Fairlamb, A.E. Goeta, A.R. Kapdi, A.L. Thompson, New J. Chem. 28 (2004) 600.
[3] (a) J. Tsuji, Palladium Reagents and Catalysts, Wiley, 2004;
(b) F. Diederich, P.J. Stang, Metal-Catalyzed Cross-Coupling Reactions, Wiley-VCH, Weinheim, 1998.
[4] A. Sundermann, J.M.L. Martin, Chem. Eur. J. 7 (2001) 1703.
[5] (a) F. Barrios-Landeros, J.F. Hartwig, J. Am. Chem. Soc. 127 (2005) 6944;
(b) A.H. Roy, J.F. Hartwig, J. Am. Chem. Soc. 125 (2003) 13944;
(c) C. Amatore, A. Jutand, Acc. Chem. Res. 33 (2000) 314;
(d) C. Amatore, A. Jutand, J. Organomet. Chem. 576 (1999) 254;
(e) A.L. Casado, P. Espinet, Organometallics 17 (1998) 954;
(f) A. Jutand, A. Mosleh, Organometallics 14 (1995) 1810;
(g) J.F. Hartwig, F. Paul, J. Am. Chem. Soc. 117 (1995) 5373;
(h) F. Paul, J. Patt, J.F. Hartwig, Organometallics 14 (1995) 3030;
(i) C. Amatore, A. Jutand, A. Suarez, J. Am. Chem. Soc. 115 (1993) 9531;
(j) M. Portnoy, D. Milstein, Organometallics 12 (1993) 1665;
(k) C. Amatore, F. Pflüger, Organometallics 9 (1990) 2276.
[6] (a) M. Ahlquist, P. Fristrup, D. Tanner, P.-O. Norrby, Organometallics 25 (2006) 2066;
(b) S. Kozuch, C. Amatore, A. Jutand, S. Shaik, Organometallics 24 (2005) 2319;
(c) L.J. Goossen, D. Koley, H.L. Hermann, W. Thiel, Organometallics 24 (2005) 2398;
(d) L.J. Goossen, D. Koley, H.L. Hermann, W. Thiel, Chem. Commun. (2004) 2141.
[7] (a) A. Ariafard, Z. Lin, Organometallics 25 (2006) 4030;
(b) A. Diefenbach, G.T. de Jong, F.M. Bickelhaupt, J. Chem. Theory Comput. 1 (2005) 286;
(c) H.M. Senn, T. Ziegler, Organometallics 23 (2004) 2980;
(d) M. Jakt, L. Johannissen, H.S. Rzepa, D.A. Widdowson, A. Wilhelm, J. Chem. Soc., Perkin Trans. 2 (2002) 576;
(e) K. Albert, P. Gisdakis, N. Rösch, Organometallics 17 (1998) 1608;
(f) F.M. Bickelhaupt, T. Ziegler, P.v.R. Schleyer, Organometallics 14 (1995) 2288.
[8] (a) M. Ahlquist, P.-O. Norrby, Organometallics 26 (2007) 550;
(b) K.C. Lam, T.B. Marder, Z. Lin, Organometallics 26 (2007) 758;
(c) A.A.C. Braga, G. Ujaque, F. Maseras, Organometallics 25 (2006) 3647;
(d) T.R. Cundari, J. Deng, J. Phys. Org. Chem. 18 (2005) 417.
[9] (a) A. Ariafard, J. Organomet. Chem. 689 (2004) 2275;
(b) G. Frenking, K. Wichmann, N. Fröhlich, J. Grobe, W. Golla, D. Le Van, B. Krebs, M. Läge, Organometallics 21 (2002) 2921;
(c) D.S. Nemcsok, A. Kovács, V.M. Rayon, G. Frenking, Organometallics 21 (2002) 5803.
[10] R.H. Crabtree, The Organometallic Chemistry of the Transition Metals, fourth ed., Wiley, New York, 2005, pp. 101–102.
[11] M.J. Frisch, G.W. Trucks, H.B. Schlegel, G.E. Scuseria, M.A. Robb, J.R. Cheeseman, V.G. Zakrzewski Jr., J.A. Montgomery, R.E. Stratmann, J.C. Burant, S. Dapprich, J.M. Millam, A.D. Daniels, K.N. Kudin, M.C. Strain, O. Farkas, J. Tomasi, V. Barone, M.C.R. Cossi, B. Mennucci, C. Pomelli, C. Adamo, S. Cliord, J. Ochterski, G.A. Petersson, P.Y. Ayala, Q. Cui, K. Morokuma, D.K. Malick, A.D. Rabuck, K. Raghavachari, J.B. Foresman, J. Cioslowski,

Ortiz, A.G. Baboul, B.B. Stefanov, G. Liu, A. Liashenko, P. Piskorz, I. Komaromi, R. Gomperts, R.L. Martin, D.J. Fox, T. Keith, M.A. Al-Laham, C.Y. Peng, A. Nanayakkara, C. Gonzalez, M. Challacombe, P.M.W. Gill, B. Johnson, W. Chen, M.W. Wong, J.L. Andres, C. Gonzalez, M. Head-Gordon, E.S. Replogle, J.A. Pople, GAUSSIAN 98 Revision A.7, Gaussian, Inc., Pittsburgh, PA, 1998.

[12] (a) A.D. Becke, J. Chem. Phys. 98 (1993) 5648;
(b) B. Miehlich, A. Savin, H. Stoll, H. Preuss, Chem. Phys. Lett. 157 (1989) 200;
(c) C. Lee, W. Yang, G. Parr, Phys. Rev. B 37 (1988) 785.

[13] (a) P.J. Hay, W.R. Wadt, J. Chem. Phys. 82 (1985) 270;
(b) W.R. Wadt, P.J. Hay, J. Chem. Phys. 82 (1985) 284;
(c) P.J. Hay, W.R. Wadt, J. Chem. Phys. 82 (1985) 299.

[14] P.C. Hariharan, J.A. Pople, Theor. Chim. Acta 28 (1973) 213.

[15] S. Huzinaga, Gaussian Basis Sets for Molecular Calculations, Elsevier, Amsterdam/New York, 1984, p. 70.

[16] E.D. Glendening, A.E. Read, J.E. Carpenter, F. Weinhold, NBO (version 3.1), Gaussian, Inc., Pittsburg, PA, 1998.

[17] A.W. Ehlers, M. Bohme, S. Dapprich, A. Gobbi, A. Hollwarth, V. Jonas, K.F. Kohler, R. Stegmann, A. Veldkamp, G. Frenking, Chem. Phys. Lett. 208 (1993) 111.

[18] (a) A. Bergner, M. Dolg, W. Kuechle, H. Stoll, H. Preuss, Mol. Phys. 80 (1993) 1431;
(b) M. Dolg, U. Wedig, H. Stoll, H. Preuss, J. Chem. Phys. 86 (1987) 866.

[19] S. Dapprich, G. Frenking, J. Phys. Chem. 99 (1995) 9352.

[20] S. Dapprich, G. Frenking, CDA 2.1, Marburg, Germany, 1994.

[21] Contrary to the case of PCl_3, the rotational conformation of the PMe_3 ligands in **1TS_Me** is nearly eclipsed. One of the reviewers was concerned that a staggered conformation of the PMe_3 groups in **1TS_Me** might stabilize the transition state more when compared to an eclipsed conformation of the PMe_3 groups. On the basis of our calculations, such a transition state does not correspond to a saddle point on the potential energy surface and attempts to locate the transition state led to **1TS_Me** with an eclipsed conformation. The result is understandable because the oxidative addition of PhBr to $Pd(PMe_3)_2$ has an early transition state. Thus, the steric repulsion between two PMe_3 groups cannot play a crucial role in the reactivity.

[22] (a) A. Diefenbach, G.T. de Jong, F.M. Bickelhaupt, J. Chem. Theory Comput. 1 (2005) 286;
(b) A. Diefenbach, F.M. Bickelhaupt, J. Phys. Chem. A 108 (2004) 8640;
(c) F.M. Bickelhaupt, J. Comput. Chem. 20 (1999) 114.

[23] H. Urata, M. Tanaka, T. Fuchikami, Chem. Lett. (1987) 751.

[24] (a) C. Boehme, G. Frenking, Organometallics 17 (1998) 5801;
(b) J. Uddin, S. Dapprich, G. Frenking, B.F. Yates, Organometallics 18 (1999) 457.

[25] (a) J.-P. Corbet, G. Mignani, Chem. Rev. 106 (2006) 2651;
(b) M.-D. Su, S.-Y. Chu, Chem. Phys. Lett. 282 (1998) 25;
(c) A. Yammamoto, T. Yammamoto, F. Ozawa, Pure Appl. Chem. 57 (1985) 1799.

[26] (a) T. Matsubara, Organometallics 22 (2003) 4286;
(b) D.S. McGuinness, K.J. Cavell, B.F. Yates, B.W. Skelton, A.H. White, J. Am. Chem. Soc. 123 (2001) 8317;
(c) M.-D. Su, S.-Y. Chu, Inorg. Chem. 37 (1998) 3400;
(d) S. Sakaki, B. Biswas, M. Sugimoto, J. Chem. Soc., Dalton Trans. (1997) 803;
(e) M. Portnoy, D. Milstein, Organometallics 12 (1993) 1665.